



Brief communication: Rainfall thresholds based on Artificial neural networks can improve landslide early warning

Pierpaolo Distefano¹, David J. Peres^{1*}, Pietro Scandura¹ and Antonino Cancelliere¹

¹Department of Civil Engineering and Architecture, University of Catania, Catania, 95123, Italy

5 *Correspondence: David J. Peres (djperes@dica.unict.it)

Abstract. In this communication we show how the use of artificial neural networks (ANNs) can improve the performance of the rainfall thresholds for landslide early warning. Results for Sicily (Italy), show how performance of a traditional rainfall event duration and depth power law threshold, yielding a true skill statistic (TSS) of 0.50, can be improved by ANNs (TSS = 0.59). Then we show how ANNs allow to easily add other variables, like peak rainfall intensity, with a further performance improvement (TSS = 0.64). This may stimulate more research on the use of this powerful tool for deriving landslide early warning thresholds.

Introduction

Landslides triggered by rainfall can cause damage on infrastructures, buildings, and in the worst scenario, even human loss. Commonly, rainfall thresholds indicating the conditions under which a warning should be issued to protect the population from a possible landslide event, are determined using empirical methods that link characteristics of precipitation, such as duration D and mean intensity I or cumulated rainfall $H = ID$ (Guzzetti et al., 2008). Rainfall thresholds are generally determined by assuming a predetermined parametric equation, which in most of the cases is a power law. Such a constraint can potentially limit the predictive performance of the thresholds, because the informative content of the considered explanatory variables may not be exploited at fullest. Artificial Neural Networks (ANNs), belonging to Artificial intelligence or Machine learning techniques, are a very flexible tool, that allow to potentially remove the mentioned limitation of predetermined parametric threshold forms, as they are capable to reproduce a vast range of non-linear classifiers (Haykin, 1999).

Up to now, a number of studies have used the potentiality of ANNs and of other machine learning techniques in landslide risk analysis. Many studies focused on susceptibility mapping and individual slope instability have exploited the potentialities of ANNs. For instance, Ermini et al. (2005) created a susceptibility map for Riomaggiore (Italy), comparing two different types of ANNs: Multilayer Perceptions (MLP) and a Probabilistic Neural Networks (PNN). Melchiorre et al. (2008) used neural networks in combination with cluster analysis for automatically splitting the available dataset in training and validation subsets, with the aim of deriving improved susceptibility maps. Other studies focus on similar applications, taking into account other variables, such as topographic wetness index (TWI) and stream power index (SPI) (Conforti et al., 2014) or the sediment transport index (STI) and the NDVI (Normalized Difference Vegetation Index), using up to 14 different input variables as



30 predisposing factors (He et al., 2019). Finally, in a recent study, Napoli et al. (2021) used ANNs to map landslide susceptibility
based on nine predisposing factors, and then combined the results with a simplified model for landslide runout prediction. In
other studies, the focus is on the prediction of individual deep seated landslide displacements by machine-learning algorithms
using detailed in situ data (Cao et al., 2016; Krkač et al., 2017; Miao et al., 2018). Among these applications, recently van
Natiijne et al. (2020) described and listed the available parameters for displacement prediction from radar and remote sensing
35 technology (slope, geology, soil moisture, precipitation/snow melt, land use), and how they may be used within a local early
warning system based on machine learning techniques, such as ANNs.

As shown in this short literature review, ANN skills are used to create susceptibility maps and/or in local early warning
systems, while application for territorial landslide early warning (Piciullo et al., 2018) has not been investigated so far. In this
communication we present our preliminary investigations showing how ANNs can allow to derive landslide early warning
40 thresholds with higher performances than traditional rainfall duration – depth power law thresholds.

Data and methods

We refer to the case study of Sicily, one of the 20 regions of Italy (Fig. 1). We have retrieved hourly rainfall from 306 rain
gauges distributed within the region, managed by the Regional water observatory (Osservatorio delle Acque, OdA), the SIAS
(Sicilian Agro-meteorological Information Service), and by the Regional Civil Protection Department (DRPC). Fig. 1 shows
45 the rain gauge locations for the period 2009-2018 (red dots) and those available only for the period 2014-2018 (black dots).

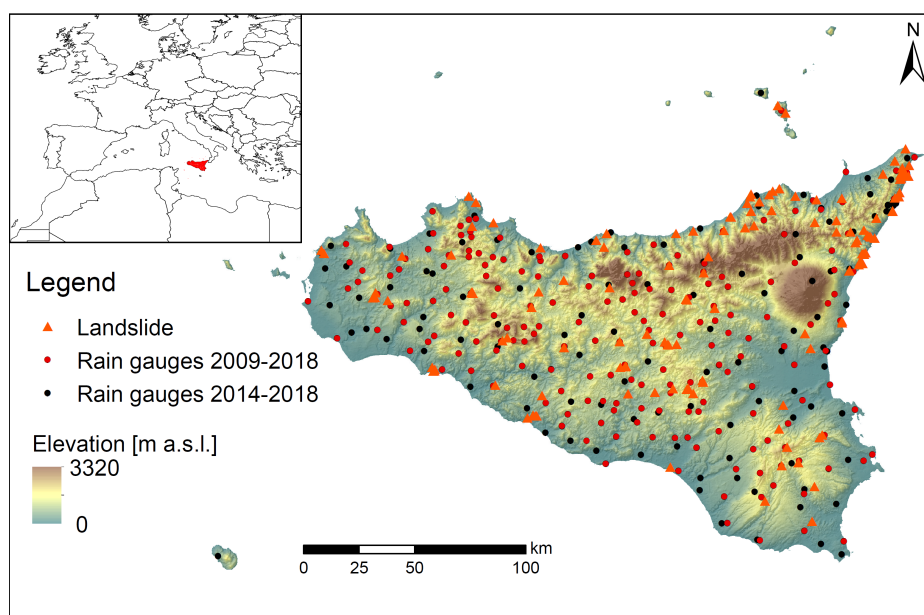


Figure 1: Elevation map showing location of landslides and rain gauges in Sicily used in this study. The rainfall dataset was built by joining dataset managed by different authorities and landslides from the Franeitalia inventory (Calvello and Pecoraro, 2018).



50

Landslides data comes from the FraneItalia database compiled by Calvello and Pecoraro (2018) – see locations on Fig. 1. This database originally contained information on landslides occurred in Italy from January 2010 to December 2017. The database has been recently updated with landslides occurred in 2018-2019 (<https://franeitalia.wordpress.com/database/>, last accessed on 29/06/2021). The information within this data base concern landslides triggered by rain but also those triggered by anthropogenic causes and earthquakes.

55

A flow chart of the applied methodology is shown in Fig. 2a. After collecting the data, some preprocessing has been carried out. In particular, landslides triggered by different precursors than rainfall were removed from our analysis. Also, suspicious rainfall data has been removed. In particular, where hourly rainfall exceeded 250 mm – corresponding to about one third of mean yearly rainfall for Sicily – the series has been visually inspected, and in the case of an evident error (rain gauge malfunction) the whole rainfall event surrounding the peak has been removed.

60

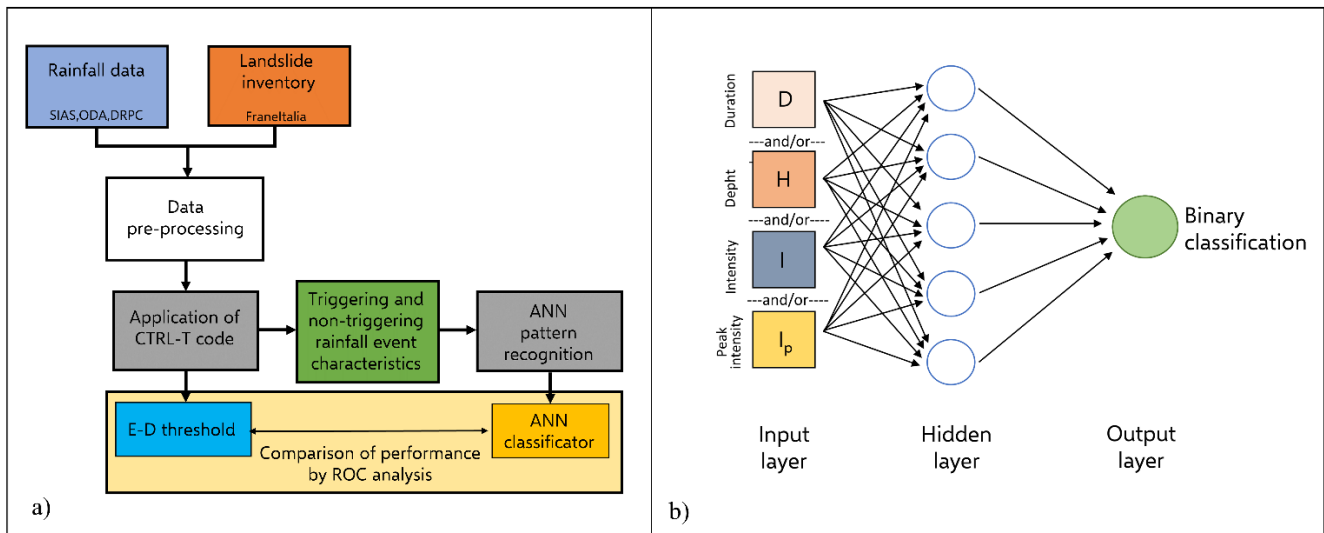


Figure 2: Flow chart illustrating the methodology (a) and the Artificial neural network architecture considered (b).

65 Pre-processed precipitation and landslide data were inputted to the CTRL-T (Calculation of Thresholds for Rainfall-induced Landslides-Tool) code (Melillo et al., 2015; 2018). The software consists of a code in R language, and allows to reconstruct rainfall events and characterizing them by the following variables: duration D , mean intensity I , total depth $H = D I$ and peak intensity I_p (defined as the maximum hourly intensity occurring during a rainfall event). The most probable rainfall conditions associated to each landslide (multiple rain gauges available for a given location) event are computed by the software based on distance between rain gauge and the landslide location, and the characteristics of the reconstructed rainfall event. Finally, the code provides power-law H - D thresholds for different levels of non-exceedance frequency of triggering events. The software

70



allows the user to set different values of the parameters to reconstruct rainfall events in order to take into account seasonality, i.e. different average evapotranspiration rates in different periods of the year. In particular, following the study by Melillo et al. (2016), we assumed that in the warm season C_w (April – October) the minimum dry period separating two rainfall events is of $P_{4warm} = 48$ hours, while in the cold season a longer period is assumed ($P_{4cold} = 96$ hours). The rain gauge sensitivity is $G_s = 0.1$ mm. A binary coding has been attributed each rainfall events, flagging triggering events as a target with value of 1 and a non-triggering event with null value. Application of the CTRL-T software yielded 144 triggering rainfall events and 47398 non-triggering events.

The characteristics of the events were used as input variables to ANNs devised for pattern recognition, as implemented within the Neural Net Pattern Recognition tool in MATLAB. The neural network, characterized by a feed-forward structure (Fig 2b), is composed of three layers: input, hidden and output. Two different activation functions have been considered: a tan-sigmoid function $f(n)$ for the hidden layer, and a log-sigmoid $g(n)$ for the output layer:

$$f(n) = \frac{2}{(1+e^{-2n})} - 1 \quad (1)$$

$$g(n) = \frac{1}{(1+e^{-n})} \quad (2)$$

The entire dataset of rainfall events was divided into a training, a validation, and a test data set, selected randomly from the entire dataset, in the proportions of 70%, 15% and 15%. This subdivision allowed to apply the early-stopping criterion to prevent overfitting. According to this criterion, the training of the neural network is stopped when the values of the performance function calculated on the validation dataset start to get worse. The ANNs have been trained through the scaled conjugate gradient backpropagation algorithm, while cross-entropy was assumed as the performance function for training. Denoting the generic ANN output with y_i (assuming values in the open interval between 0 and 1) and the binary target with t_i , $i=1,2, \dots, N$, the cross-entropy function F heavily penalizes inaccurate predictions and assigns minimum penalties for correct predictions:

$$F = -\frac{1}{N} \sum_{i=1}^N [t_i \log y_i + (1 - t_i) \log(1 - y_i)] \quad (3)$$

The ability to distinguish triggering events from non-triggering events was measured using the confusion matrix, a double-entry table in which it is possible to identify true positive TP (triggering events correctly classified), true negative TNs (non-triggering events correctly classified), the false negative FN (triggering events classified as non-triggering) and FP false positive (non-triggering events classified as triggering). Using the confusion matrix it is possible to determine the True Positive Rate and the False Positive Rate, as well as their difference, known as the True skill statistic, which is widely used for threshold determination (Peres and Cancelliere, 2021):

$$TPR = \frac{TP}{TP+FN} \quad (4)$$

$$FPR = \frac{FP}{TN+FP} \quad (5)$$

$$TSS = TPR - FPR \quad (6)$$

For our analysis different combination of input data (duration D , intensity I , total depth H and peak intensity I_p) and different architectures, changing number of hidden neurons were tested. The output of the ANNs is transformed into a binary code, by



the application of a threshold. Varying the threshold, a Receiver-Operating Characteristics (ROC) curve is derived (TPR vs
105 FPR), and the threshold maximizing TSS is identified.

Results from ANNs are compared with rainfall duration-depth power-law thresholds derived through the maximization of TSS
– i.e., again, analysing both triggering and non-triggering events.

Results and discussion

Application of the CTRL-T software has allowed to build the dataset of triggering and non-triggering events and to derive the
110 threshold according to the so-called frequentist method (based on triggering events only). Considering a non-exceedance
frequency for triggering events equal to 5%, threshold from the software is as follows:

$$H = 4.9D^{0.26} \quad (7)$$

This threshold is lower than the one obtained for Sicily by Gariano et al. (2015), yet comparable with an updated one derived
by Melillo et al., (2016) through an earlier version of the algorithm that was then implemented by CTRL-T software.
115 Specifically, thresholds reported on the mentioned two studies are respectively the following (non-exceedance frequency is
again 5%):

$$H = 10.4D^{0.27} \quad (8)$$

$$H = 5.6 D^{0.40} \quad (9)$$

These thresholds however are not comparable with those to derive with the proposed ANN approach, because non-triggering
120 events are neglected. We have hence derived the power-law threshold corresponding to the maximum TSS, obtaining the
following result:

$$H = 2.40D^{0.68} \quad (10)$$

that has a $TSS = TSS_0 = 0.50$. The threshold has a lower intercept but a higher slope, so, after a duration of about 5 hours, it is
above that the one given in Eq. 7.

125 For the derivation of thresholds based on ANNs, the following input variable configurations have been investigated: 1) D ; 2)
 H ; 3) I ; 4) I_p ; 5) D and H ; 6) D and I ; 7) D and I_p ; 8) H and I_p ; 9) I and I_p ; 10) D , H and I_p . The listed input configurations are
indeed all possible ones, except those combining both H and I with duration D . This has been done because the two pairs D - I
and D - H have the same informative content by construction, as confirmed by the fact that the performances of the D - I and D -
 H neural networks do not differ significantly (see later, Tab. 1). All the data have been inputted taking their natural logarithms.
130 Different networks have been considered varying the number of hidden neurons from 5 to 20, in order to search for the best
value, i.e., the one yielding the highest TSS. Table 1 shows the results obtained from the tested 160 neural network
configurations. In particular, the table shows, for each set of input variables: the optimal number of hidden neurons
corresponding to the maximum TSS for the entire data set (third column). The subsequent columns of the table show the TSS
for the training, validation and test data sets, with respect to the reported number of hidden neurons. As can be seen, for most
135 of the input configurations, the TSS for the test and validation data sets is generally quite close, if not greater than the TSS in



the training data set. This proves that overfitting has been sufficiently prevented, thanks to the early-stopping criterion – otherwise the performance in the training data set would have been significantly higher than those in the test data set. Hence, in the following discussion we will refer to the TSS computed on the entire data set.

140 **Table 2: Results of tests with ANNs, showing the optimal number of hidden neurons (a number from 5 to 20 has been tested) and the True skill statistics (TSS) for the entire, the training, the validation and the test data sets. Values in the table are compared to $TSS_0 = 0.50$ which is the maximum value associated to a $D-H$ power law threshold.**

Input data	Hidden neurons (max TSS)	TSS all	TSS training	TSS validation	TSS test
D	5	0.30	0.33	0.32	0.21
H	18	0.42	0.41	0.43	0.50
I	20	0.45	0.44	0.57	0.47
I_p	14	0.36	0.36	0.42	0.37
$D-H$	14	0.59	0.63	0.53	0.67
$D-I$	6	0.59	0.57	0.72	0.69
$D-I_p$	10	0.50	0.51	0.55	0.47
$H-I_p$	15	0.43	0.48	0.45	0.36
$I-I_p$	20	0.58	0.60	0.64	0.53
$D-H-I_p$	17	0.64	0.65	0.67	0.61

As can be seen from the Table, using only one input variable, the performances are significantly lower than those obtained from the use of the power-law threshold of Eq. 10: however, for the variable with the highest informative content, mean rainfall intensity I , the TSS = 0.45 is quite close to $TSS_0 = 0.50$. When using input variables in pairs, performances increase significantly. Notably, in the case of the pairs $D-I$ and $D-H$ – i.e., the same variables used for the power law – the TSS = 0.59, which is significantly higher than TSS_0 . The fact that with same input data the neural network provides significantly better performances than the power law, proves that the use of a predetermined parametric form for the threshold equation does not allow to exploit at the fullest the informative content of the input variables, while the flexibility of ANNs allows to achieve a better classification.

Finally, adding a third variable (network input $D-H-I_p$), a further improvement is obtained (TSS = 0.64). This result demonstrates how neural networks can be an aid in searching additional variables that can provide a more reliable dynamic prediction of landslide triggering conditions. In particular, in this case, it has been shown that peak intensity may have an important informative content, an aspect that has not been perhaps sufficiently investigated in the literature.

Conclusions

The identification of rainfall thresholds indicating landslide triggering conditions is a key step for implementing territorial landslide early warning systems. Commonly, thresholds are searched in a limited space, i.e., constrained to a predetermined



parametric form, which is generally a power law linking rainfall event, duration D and mean intensity I (or total depth $H = D$
160 J). In this communication we have shown that choosing a predetermined form for the law of the threshold can potentially limit
the performance of the empirical model, and how Artificial neural networks are a valuable tool to overcome this limitation.
The analysis, referred to the case study of Sicily, has shown that an H - D power-law threshold has a maximum true skill statistic
of $TSS = TSS_0 = 0.50$. On the other hand, the classifier based on neural networks, using the same pair of input variables,
yielded a significantly greater $TSS = 0.59$. It has also been shown how neural networks allow to easily explore the potential
165 information content of other variables, and hence provide a way to improve predictive performance. For instance, it has been
shown that the inclusion of peak rainfall intensity as an additional variable, can lead to an improvement of performance. It is
important that when training neural networks, generalization capabilities are ensured, for instance by the early stopping
technique. Overfitting is not an issue for the traditional approach based on the power law – or any other parametric equation –
as in general the number of free parameters is very low (2 for a power law). This may be a drawback for neural networks, even
170 though it forces one to consider both triggering and non-triggering events, which is fundamental for obtaining thresholds with
acceptable statistical characteristics (Peres and Cancelliere, 2021). Another possible disadvantage of neural networks with
respect to predetermined-form thresholds is also represented by the fact that it is generally not possible to summarize the neural
network classifier as a simple equation. This could hamper the practical implementation of triggering thresholds based on
neural networks, which could be perceived as impractical. However, this limit can potentially be overcome by providing a
175 user-friendly software to the end user.

Data availability. Landslide data from the FraneItalia database (Calvello and Pecoraro, 2018) are available from
<https://franeitalia.wordpress.com/database/> (last accessed on 29/06/2021), while part of the rainfall data is available from
websites of the Servizio Informativo Agrometeorologico Siciliano (SIAS) (<http://www.sias.regione.sicilia.it/>, last accessed
on 05/07/2021) and the Osservatorio delle Acque (<http://www.osservatorioacque.it/>, last accessed on 05/07/2021).

180 **Acknowledgements.** Pierpaolo Distefano doctoral program’s grant is funded by the “Notice 2/2019 for financing the Ph.D.
regional grant in Sicily” as part of the Operational Program of European Social Funding 2014–2020 (PO FSE 2014–2020)
CUP E65E19000830002. David J. Peres was supported by the post-doctoral grant on “Sviluppo di modelli per la valutazione
di strategie innovative di gestione delle risorse idriche in un contesto di cambiamenti climatici” (Development of models for
the evaluation of new strategies for water resources management in a changing climate). The research has been partially
185 conducted within the following projects: LIFE 17 CCA/IT/000115 SimetoRES funded by the EASME (now CINEA) of the
European Commission, and the Programma Operativo Nazionale Governance e Capacità Istituzionale 2014-2020 - Programma
per il supporto al rafforzamento della governance in materia di riduzione del rischio ai fini di protezione civile CUP (Program
to support the strengthening of governance in the field of risk reduction for civil protection purposes). APCs funded by “fondi
di ateneo 2020-2022, Università di Catania, linea Open Access”.

190 References

Calvello, M. and Pecoraro, G.: FraneItalia: a catalog of recent Italian landslides, *Geoenvironmental Disasters*, 5(1),
doi:10.1186/s40677-018-0105-5, 2018.

Cao, Y., Yin, K., Alexander, D. E. and Zhou, C.: Using an extreme learning machine to predict the displacement of step-like



- landslides in relation to controlling factors, *Landslides*, 13(4), 725–736, doi:10.1007/s10346-015-0596-z, 2016.
- 195 Conforti, M., Pascale, S., Robustelli, G. and Sdao, F.: Evaluation of prediction capability of the artificial neural networks for mapping landslide susceptibility in the Turbolo River catchment (northern Calabria, Italy), *CATENA*, 113, 236–250, doi:10.1016/J.CATENA.2013.08.006, 2014.
- Ermini, L., Catani, F. and Casagli, N.: Artificial Neural Networks applied to landslide susceptibility assessment, *Geomorphology*, 66(1–4), 327–343, doi:10.1016/J.GEOMORPH.2004.09.025, 2005.
- 200 Gariano, S. L., Brunetti, M. T., Iovine, G., Melillo, M., Peruccacci, S., Terranova, O., Vennari, C. and Guzzetti, F.: Calibration and validation of rainfall thresholds for shallow landslide forecasting in Sicily, southern Italy, *Geomorphology*, 228, 653–665, doi:10.1016/J.GEOMORPH.2014.10.019, 2015.
- Guzzetti, F., Peruccacci, S., Rossi, M. and Stark, C. P.: The rainfall intensity-duration control of shallow landslides and debris flows: An update, *Landslides*, 5(1), 3–17, doi:10.1007/s10346-007-0112-1, 2008.
- 205 Haykin, S.: *Neural Networks- A Comprehensive Foundation* 2nd Ed. Prentice Hall., 1999.
- He, Q., Shahabi, H., Shirzadi, A., Li, S., Chen, W., Wang, N., Chai, H., Bian, H., Ma, J., Chen, Y., Wang, X., Chapi, K. and Ahmad, B. Bin: Landslide spatial modelling using novel bivariate statistical based Naïve Bayes, RBF Classifier, and RBF Network machine learning algorithms, *Sci. Total Environ.*, 663, 1–15, doi:10.1016/j.scitotenv.2019.01.329, 2019.
- Krkač, M., Špoljarić, D., Bernat, S. and Arbanas, S. M.: Method for prediction of landslide movements based on random forests, *Mach Learn*, 14(3), 947–960, doi:10.1007/s10346-016-0761-z, 2017.
- Melchiorre, C., Matteucci, M., Azzoni, A. and Zanchi, A.: Artificial neural networks and cluster analysis in landslide susceptibility zonation, *Geomorphology*, 94(3–4), 379–400, doi:10.1016/J.GEOMORPH.2006.10.035, 2008.
- Melillo, M., Brunetti, M. T., Peruccacci, S., Gariano, S. L. and Guzzetti, F.: An algorithm for the objective reconstruction of rainfall events responsible for landslides, *Landslides*, 12(2), 311–320, doi:10.1007/s10346-014-0471-3, 2015.
- 215 Melillo, M., Brunetti, M. T., Peruccacci, S., Gariano, S. L. and Guzzetti, F.: Rainfall thresholds for the possible landslide occurrence in Sicily (Southern Italy) based on the automatic reconstruction of rainfall events, *Landslides*, 13(1), 165–172, doi:10.1007/s10346-015-0630-1, 2016.
- Melillo, M., Brunetti, M. T., Peruccacci, S., Gariano, S. L., Roccati, A. and Guzzetti, F.: A tool for the automatic calculation of rainfall thresholds for landslide occurrence, *Environ. Model. Softw.*, 105, 230–243, doi:10.1016/J.ENVSOF.2018.03.024, 220 2018.
- Miao, F., Wu, Y., Xie, Y. and Li, Y.: Prediction of landslide displacement with step-like behavior based on multialgorithm optimization and a support vector regression model, *Landslides*, 15(3), 475–488, doi:10.1007/s10346-017-0883-y, 2018.
- Napoli, M. Di, Martire, D. Di, Bausilio, G., Calcaterra, D., Confuorto, P., Firpo, M., Pepe, G. and Cevasco, A.: Rainfall-Induced Shallow Landslide Detachment, Transit and Runout Susceptibility Mapping by Integrating Machine Learning Techniques and GIS-Based Approaches, *Water*, 13(4), 488, doi:10.3390/w13040488, 2021.
- 225 van Natijne, A. L., Lindenbergh, R. C. and Bogaard, T. A.: Machine learning: New potential for local and regional deep-seated landslide nowcasting, *Sensors (Switzerland)*, 20(5), 1–18, doi:10.3390/s20051425, 2020.
- Peres, D. J. and Cancelliere, A.: Comparing methods for determining landslide early warning thresholds: potential use of non-



230 triggering rainfall for locations with scarce landslide data availability, *Landslides*, (May), doi:10.1007/s10346-021-01704-7, 2021.

Piciullo, L., Calvello, M. and Cepeda, J. M.: Territorial early warning systems for rainfall-induced landslides, *Earth-Science Rev.*, 179(April 2017), 228–247, doi:10.1016/j.earscirev.2018.02.013, 2018.